Localization and function of the Kv3.1b subunit in the rat medulla oblongata: focus on the nucleus tractus solitarii

Mark L. Dallas, Lucy Atkinson, Carol J. Milligan, Neil P. Morris, David I. Lewis, Susan A. Deuchars and Jim Deuchars

School of Biomedical Sciences, Worsley Building, University of Leeds, Leeds LS2 9NQ, UK

The voltage-gated potassium channel subunit Kv3.1 confers fast firing characteristics to neurones. Kv3.1b subunit immunoreactivity (Kv3.1b-IR) was widespread throughout the medulla oblongata, with labelled neurones in the gracile, cuneate and spinal trigeminal nuclei. In the nucleus of the solitary tract (NTS), Kv3.1b-IR neurones were predominantly located close to the tractus solitarius (TS) and could be GABAergic or glutamatergic. Ultrastructurally, Kv3.1b-IR was detected in NTS terminals, some of which were vagal afferents. Whole-cell current-clamp recordings from neurones near the TS revealed electrophysiological characteristics consistent with the presence of Kv3.1b subunits: short duration action potentials (4.2 ± 1.4 ms) and high firing frequencies (68.9 ± 5.3 Hz), both sensitive to application of TEA (0.5 mM) and 4-aminopyridine (4-AP; 30 μM). Intracellular dialysis of an anti-Kv3.1b antibody mimicked and occluded the effects of TEA and 4-AP in NTS and dorsal column nuclei neurones, but not in dorsal vagal nucleus or cerebellar Purkinje cells (which express other Kv3 subunits, but not Kv3.1b). Voltage-clamp recordings from outside-out patches from NTS neurones revealed an outward K^+ current with the basic characteristics of that carried by Kv3 channels. In NTS neurones, electrical stimulation of the TS evoked EPSPs and IPSPs, and TEA and 4-AP increased the average amplitude and decreased the paired pulse ratio, consistent with a presynaptic site of action. Synaptic inputs evoked by stimulation of a region lacking Kv3.1b-IR neurones were not affected, correlating the presence of Kv3.1b in the TS with the pharmacological effects.

(Received 5 August 2004; accepted after revision 28 October 2004; first published online 4 November 2004)
Corresponding author J. Deuchars: School of Biomedical Sciences, Worsley Building, University of Leeds, Leeds LS2 9NQ, UK. Email: j.deuchars@leeds.ac.uk

The presence of a particular K^+ channel subunit can bestow specific electrophysiological characteristics onto neurones (Rudy *et al.* 1999). One such subunit is Kv3.1, which, when activated, produces sustained, 'delayed rectifier' currents with a high activation threshold and very rapid deactivation kinetics, at least in expression systems (Grissmer *et al.* 1994; Kanemasa *et al.* 1995). The Kv3.1 gene produces two splice variants, Kv3.1a and Kv3.1b (Luneau *et al.* 1991), which are both expressed in the axonal domain of the many cell populations in the CNS (e.g. hippocampal basket cells), while Kv3.1b is additionally localized to somatodendritic regions (Ozaita *et al.* 2002). The presence of the Kv3.1b subunit in the soma of some interneuronal populations in the cortex, hippocampus and spinal cord may support their ability to fire trains of short duration action potentials at very high rates (Weiser *et al.* 1995; Du *et al.* 1996; Chow *et al.* 1999; Deuchars *et al.* 2001), possibly by facilitating the recovery of Na^+ channel inactivation and minimizing the duration of the afterhyperpolarization (AHP; Erisir *et al.* 1999; Rudy & McBain, 2001). These features of interneurones are critical for maintaining activity in many brain regions, since the precise timing facilitates synchronization of oscillatory activity (Traub *et al.* 1999) and phase locking of neuronal activity (Brew & Forsythe, 1995; Wang *et al.* 1998).

While the precise cellular organization of the hippocampus and cerebellar cortex facilitates identification of the ion channel complement and distribution within specific neuronal classes (e.g. Lorincz *et al.* 2002), this is more difficult in less-ordered CNS regions. One such area is the nucleus of the solitary tract (NTS) in the dorsomedial brainstem. The NTS plays a pivotal role in maintaining many homeostatic mechanisms as it integrates information from numerous

M. L. Dallas and L. Atkinson contributed equally and significantly to the data.

 DOI: 10.1113/jphysiol.2004.073338

other brain areas, as well as peripheral structures via sensory nerves (Barraco *et al.* 1992). Many studies have examined the neurochemistry of the NTS (e.g. Maley, 1996; Lawrence & Jarrott, 1996), and others have revealed that the NTS contains neurones with diverse firing properties (e.g. Haddad & Getting, 1989; Fortin & Champagnat, 1993; Kawai & Senba, 1996, 1999; Deuchars *et al.* 2000). However, the molecular identity of ion channels that underlie the firing properties of NTS neurones has rarely been determined.

Here we report Kv3.1b subunit immunoreactivity throughout the medulla oblongata in cell somata and presynaptic terminals. Electrophysiological recordings from NTS neurones in slices provide evidence for functional roles consistent with the localization of Kv3.1b. Some of these data have been published in abstract form (Atkinson & Deuchars, 2000; Dallas *et al.* 2002, 2004).

Methods

All procedures were carried out in accordance with the UK Animals (Scientific Procedures) Act 1986, and animals were humanely killed at the end of experiments.

Immunohistochemistry

Wistar rats (150–200 g, $n = 10$) were anaesthetized intraperitoneally with Sagatal (60 mg kg^{-1}) and transcardially perfused with 4% paraformaldehdye (PFA) and between 0.05 and 0.2% glutaraldehyde (in 0.1 M phosphate buffer, PB; pH 7.4). For GABA and glutamate immunohistochemistry, Wistar rats (150–200 g, $n = 6$) were anaesthetized with intraperitoneal Sagatal (60 mg kg^{-1}) and transcardially perfused with 4% PFA/4% carbocyamide/0.05% glutaraldehdye in 0.1 M PB. The brains and/or nodose ganglia were removed and post fixed in the same solution for 2 h at 4°C. Coronal (50 μm) sections of the relevant tissues were then cut on a vibrating microtome (Leica, Milton Keynes, UK) and collected into phosphate buffered saline (PBS; pH 7.2).

Immunohistochemistry was performed by incubating sections in primary antibody raised against the end portion of the intracellular C-terminus (residues 567–585) of the rat Kv3.1b channel subunit (Alomone Laboratories, Jerusalem, Israel; 1:1000 in PBS/0.1% Triton X-100, raised in rabbit) or rat Kv3.2 (1:1000 in PBS; Alomone Laboratories) for 12–18 h at 4°C. For fluorescence, these antibodies were visualized using Cy3-conjugated antirabbit antibodies (1:1000 in PBS; Stratech Scientific, Luton, UK) for ∼4 h at room temperature. Sections were then air-dried onto slides and mounted under a coverslip using VectaMount mounting medium (Vector Laboratories, Burlingame, CA, USA).

Dual labelling. To determine the percentage of neurones that contained Kv3.1b immunoreactivity (Kv3.1b-IR), sections containing Cy3-labelled Kv3.1b-IR were incubated in a neuronal nuclear marker (NeuN) primary antibody (1:1000 in PBS; Chemicon, Hertfordshire, UK; raised in mouse) overnight at 4°C. Following washes in PBS, the sections were incubated in a biotinylated mouse secondary antibody (1:500; Stratech Scientific) for ∼4 h, washed again in PBS and then incubated in streptavidin-conjugated Alexa^{488} (1:1000; Molecular Probes) for ∼2 h. The number of NeuN-IR and Kv3.1b-IR neurones were counted in representative sections of levels of the medulla relative to the area postrema. For counting purposes the NTS was subdivided into medial (classically defined medial and commissural aspect of the tractus solitarius, TS) and lateral (encompassing the TS and surrounding subdivisions: interstitial, dorsolateral, ventrolateral, ventral, intermediate and dorsal). Dual-labelled cells were expressed as a percentage of the total number of cells. To determine the neurochemistry of Kv3.1b-IR neurones, some labelled sections were incubated in mouse anti-GABA and mouse antiglutamate (both at 1:1000 in PBS/0.1% Triton X-100; Sigma, Dorset, UK), visualized and detected as above.

Some sections were also processed for light and electron microscopy as described in detail previously (Atkinson & Deuchars, 2000). In brief, sections were incubated in anti-Kv3.1b (1:1000 in PBS) which was localized using biotinylated antirabbit secondary antibody (1:200 in PBS, Stratech Scientific) prior to detection with ExtrAvidin peroxidase (1:1500 in PBS; Sigma) and visualization using diaminobenzidine (DAB) as the chromogen. Sections were then postfixed in 0.5% osmium tetroxide (in 0.1 M PB) and dehydrated before embedding in Durcupan ACM resin (Fluka, Switzerland). Kv3.1b-IR NTS cells were drawn under the ×20 objective using a camera lucida drawing tube. Areas with suitable staining were prepared for electron microscopy, and viewed on a Phillips CM10 transmission electron microscope (EM). Negatives were digitized using an Umax 2200 scanner, and adjusted in Corel Draw 10 (Corel, Maidenhead, Berkshire, UK) until the desired brightness, contrast and gamma levels were reached.

Control sections were incubated for 12–24 h as above, either in PBS in place of the primary antibody or in primary antibody which had been preabsorbed with peptide antigen (1 μg per 1 μg of primary antibody; Alomone Laboratories) for 1 h at room temperature. These sections were then incubated in biotinylated secondary antibody, followed by ExtrAvidin peroxidase, and reacted using DAB as described previously. All control sections were free from immunoreactivity.

Vagal efferent cell and afferent fibre labelling combined with Kv3.1b immunohistochemistry

To retrogradely label vagal efferent cells, four male Wistar rats (150–250 g) were injected intraperitoneally with 100 μl of Fluorogold (2% in distilled water; Fluorochrome Inc., Denver, CO, USA) 7 days prior to perfusion. Vagal afferent fibres were labelled by injection of 5–10 μl of 10% biotinylated dextran amine (BDA, molecular mass 10 000 kDa; Molecular Probes) into the right nodose ganglion of seven Wistar rats (150–250 g) under halothane anaesthesia (5% in O_2) 7–10 days prior to perfusion and sectioning as described previously. BDA was visualized using ExtrAvidin peroxidase and a DAB reaction, while anti-Kv3.1b antibodies were visualized using pre-embedding gold procedures (Atkinson *et al.* 2000).

Kv3.1b-IR and GAD_{65}/VGLUT2 *in situ* hybridization in the NTS

Wistar rats (150–200 g, $n = 6$) were anaesthetized with intraperitoneal sagatal (60 mg kg^{-1}), perfused transcardially with 4% PFA, and coronal (30 μm) sections of the medulla were cut as described previously. *In situ* hybridization was conducted using previously published protocols (Stornetta *et al.* 2002). To visualize GABAergic neurones single-stranded digoxigenin (DIG)-UTP-labelled (Roche Molecular Biochemicals, Switzerland) sense (control) and antisense riboprobes were transcribed from a 2.3 kb GAD_{65} DNA template plasmid kindly supplied and previously characterized by A. Tobin (Wuenschell *et al.* 1986; Esclapez *et al.* 1993). For glutamatergic neurones, sense and antisense VGLUT2 riboprobes were transcribed from a 3.3 kb DNA template kindly supplied and previously characterized by R. Stornetta (Stornetta *et al.* 2002). Hybridized mRNA was visualized with nitroblue tetrazolium chloride and 5-bromo-4-chloro-3-indolyl phosphate (NBT/BCIP) diluted in Tris-HCl/$MgCl_2$, pH 9.5. The sections were then incubated in Kv3.1b primary antibody (1:500) for 12–18 h at 4°C, washed for 3×10 min in PBS, and visualized by incubation in a Cy3-conjugated secondary antibody as described previously.

Image capture

Slides were viewed on a Nikon E600 microscope equipped with epifluorescence. Images were captured directly from the slide using an Aquis Image Capture system (Synoptics, Cambridge, UK), and adjusted in CorelDraw 10 until the desired gamma, brightness and contrast levels were reached.

RT-PCR

Wistar rats (150–200 g, n = 5) were anaesthetized with Sagatal (60 mg kg^{-1}), and transcardially perfused with artificial cerebrospinal fluid (aCSF). The medulla and nodose ganglia were removed, and RNA was isolated from these tissues using TRI reagent (according to the manufacturer's instructions). RT-PCR was then performed using the Kv3.1 primers (sense: 5′-CAAGAGATTGGCGCTCAGTGAC-3′, antisense: 5′-CCCAGRGCCAGRAAGATGATMAGCA-3′) which detects a 584 bp sequence of the Kv3.1 channel corresponding to the amino acid sequence 153–354. The PCR cycling conditions were: 94°C for 5 min, 94°C for 45 s, 57°C for 30 s, 72°C for 45 s for 35 cycles. The RT-PCR product was then run on a 2% agarose gel and viewed under a Hybaid Illuminator.

Electrophysiological experiments

Slice preparation. Wistar rats (18–21 days) were terminally anaesthetized with intraperitoneal sodium pentobarbitone (120 mg kg^{-1}). The brain was removed and placed in ice-cold sucrose aCSF containing (mM): sucrose (217); $NaHCO_3$ (26); KCl (3); $MgSO_4$ (2); NaH_2PO_4 (2.5); $CaCl_2$ (2); and glucose (10); that received a continual supply of mixed gas (95% O_2, 5% CO_2). Slices (300 μm) of the medulla and cerebellum were cut using a Vibroslice (Campden Instruments, Sileby, UK) and transferred to a holding chamber containing aCSF (mM): NaCl (124); $NaHCO_3$ (26); KCl (3); $MgSO_4$ (2); NaH_2PO_4 (2.5); $CaCl_2$ (2); glucose (10); equilibrated with 95% O_2, 5% CO_2. Visualized patch-clamp recordings were carried out at room temperature using an upright microscope with DIC optics (BX50WI; Olympus Optical, Tokyo, Japan). Patch electrodes were filled with intracellular solution consisting of (mM): potassium gluconate (110); EGTA (11); $MgCl_2$ (2); $CaCl_2$ (0.1); Hepes (10); Na_2ATP (2); NaGTP (0.3); and had a resistance of 6 MΩ. In some experiments, Lucifer yellow (0.1%) and/or the primary antibody raised against Kv3.1b (1:1000; Alomone Laboratories), or a primary antibody raised against the hyperpolarization-activated cyclic nucleotide-gated K^+ channel 1 subunit (HCN1, 1:1000; Alomone Laboratories) were added to the intracellular solution.

Current-clamp mode recordings

Whole-cell patch-clamp recordings were made in current-clamp mode using an Axopatch ID (Axon Instruments) from neurones ventral, and immediately adjacent to, the TS at the level of the area postrema, where the majority of Kv3.1b-IR neurones are situated. In particular, larger neurones with proximal dendrites running horizontally were selected (Fig. 2*E*) as their morphological characteristics corresponded to those of Kv3.1b-IR neurones detected by immunohistochemical experiments. Neurones were characterized as previously been described (Deuchars *et al.* 2001), following which depolarizing current pulses (+10 to +300 pA) were

applied to examine the firing properties of the neurones. Tetraethylammonium chloride (TEA; 0.5 mM) and 4-aminopyridine (4-AP; 30 μM) (both from Sigma) were applied to the bathing medium at the rate of 3–5 ml min^{-1}. While TEA may act at other channels at this concentration, overlapping sensitivity to both drugs strongly suggests an action on Kv3.1 subunits (Coetzee *et al.* 1999; Deuchars *et al.* 2001). To investigate the presynaptic actions of 4-AP and TEA, a bipolar stimulating electrode (voltage 9–18 V, duration 100 μs; model DS2A; Digitimer, Hertfordshire, UK) was placed in the TS to evoke postsynaptic potentials within NTS neurones. Recordings were carried out in current-clamp mode since we were particularly interested in how the drugs affected the firing characteristics of the neurones. Consequently, measurements of the electrophysiological characteristics were made as has previously been described (Deuchars *et al.* 2001). In addition, firing patterns were analysed in response to 1 s depolarizing current pulses, and early accommodation was calculated using the following equation: (instantaneous frequency – frequency at 500 ms)/instantaneous frequency. Late accommodation was calculated as follows: (frequency at 500 ms–frequency at 1000 ms)/instantaneous frequency.

The effects of drugs were determined using the paired *t* test on the action potential durations, amplitudes, AHP amplitudes and firing frequencies in response to depolarizing current pulses, pre- and postapplication of drugs. Differences were considered significant when $P < 0.05$. All values are stated as the mean ± the standard error mean, where n equals the number of neurones recorded from.

Voltage-clamp recordings

To isolate outward voltage-dependent K^+ currents, tetrodotoxin (TTX; 1 μM; Sigma) was bath applied, and the Ca^{2+} was replaced with magnesium (4 mM) in the aCSF. Preliminary experiments revealed a low-threshold outward delayed rectifier K^+ current characteristic of that carried by Kv1 channels, so in addition alpha-dendrotoxin (α-DTX; 100 nM; Alomone) was bath applied. Outside-out somatic patches were obtained from NTS neurones from the same location as those used for current-clamp recordings. Series resistance in the patches (18.2–20.8 MΩ, mean 19.4 ± 0.92 MΩ) was monitored periodically, and compensated (60–80%) throughout. Where the series resistance increased to a value greater than 30 MΩ, or was unstable, recordings were discontinued. Recordings were corrected for a liquid junction potential of −14.4 mV, as calculated using Clampex 8.1 software. Currents were leak subtracted online using a P/4 subtraction protocol from a holding potential of −110 mV. Signals were low-pass filtered at 5 kHz (four-pole Bessel), and sampled at 50 kHz. K^+ currents recorded from the outside-out patches are an average of five trials recorded at each voltage step. K^+ conductance (G_v)–voltage curves were fitted using Kaleidograph software with a single, first-order Boltzmann function of the form: $G_v = G_{max}/\{1 + \exp[-(V - V_{½})/k]\}$, where V is the membrane voltage, $V_{½}$ is the half-activation voltage, and k is the slope factor. Offline analysis was carried out using the Clampfit 8.1 analysis package.

Results

Kv3.1b subunit immunoreactivity in the medulla

At the levels studied (~1.3 mm rostral to 0.4 mm caudal to the obex), Kv3.1b subunit immunoreactivity (Kv3.1b-IR) was observed in a large number of medullary areas (Fig. 1*A*), where it was present in the somatic membrane and proximal dendrites of neurones, with limited labelling of dendritic arborizations, similar to that described in the cortex (Sekirnjak *et al.* 1997). Dual immunohistochemistry for the Kv3.1b subunit and the neuronal nuclear antibody NeuN revealed that Kv3.1b-IR was present in 100% of neurones in the cuneate (408/408) and gracile (530/530) nuclei (Fig. 1*B* and *C*). A low number of Kv3.1b-IR cells were observed in the vicinity of the nucleus ambiguus; however, these Kv3.1b-IR cells were not vagal efferent neurones, as they were not labelled following intraperitoneal injection of Fluorogold (Fig. 1*E*). Kv3.1b-IR was observed in 100% of the densely packed neurones in the paratrigeminal (240/240) and spinal trigeminal nuclei (Fig. 1*F*, 1240/1240). Approximately 98% of neurones in the raphe obscurus nucleus were also Kv3.1b-IR (63/63). Extremely rare Kv3.1b-IR somata were present in the hypoglossal nucleus, but these never contained Fluorogold and were therefore unlikely to be motoneurones (not shown). Somatic Kv3.1b-IR was not observed in the dorsal vagal motor nucleus (DVN; Fig. 6*C*), the inferior olive, raphe pallidus or the area postrema. In these areas, punctate Kv3.1b-IR was observed suggestive of terminal labelling, and such punctate labelling was also observed in the hypoglossal nucleus (Fig. 1*G*).

Kv3.1b-IR cells in the NTS are predominantly within the vicinity of the TS

Kv3.1b-IR was present in approximately 13% (111/825) of NeuN-labelled NTS neurones. The soma of Kv3.1b-IR neurones were predominantly round or elongated, and ranged from 25 to 50 μm in length. Kv3.1b-IR neurones also had visible proximal dendrites that ran predominantly in the mediolateral axis. Camera lucida mapping revealed that Kv3.1b-IR NTS neurones were primarily located in the vicinity of the TS. Caudally (at the level of the central canal) a few Kv3.1b-IR neurones were observed in

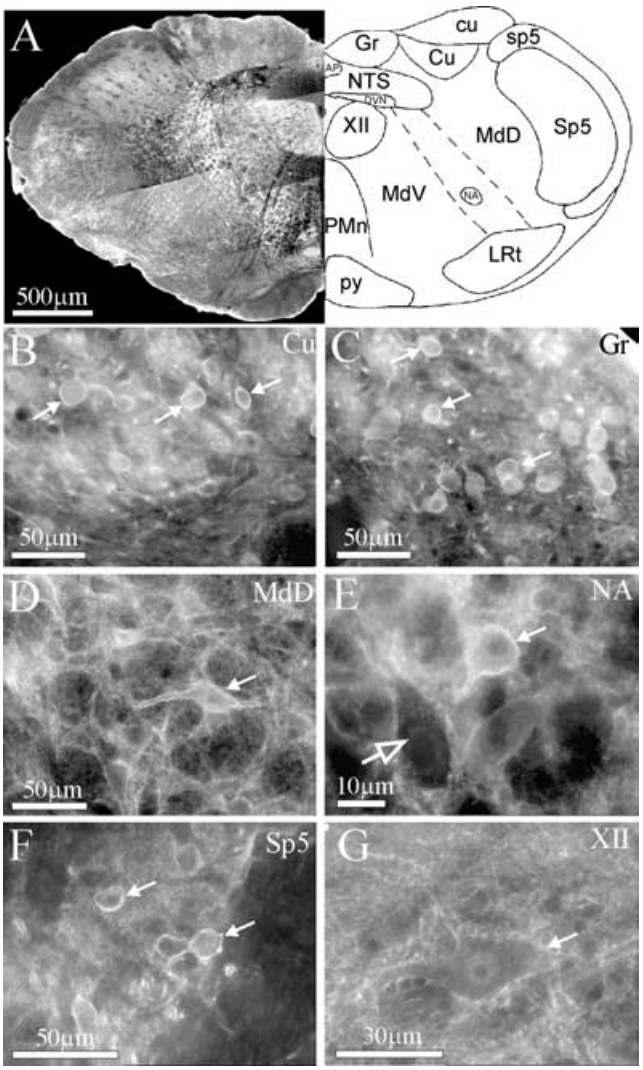

Figure 1. Kv3.1b immunoreactivity is widely distributed throughout the medulla oblongata
A, a low-power montage of Kv3.1b subunit immunoreactivity (Kv3.1b-IR) in the medulla oblongata (detected using a Cy3-conjugated secondary antibody; left-hand side) indicating that Kv3.1b-IR is present in many regions of the medulla oblongata. The right-hand side is a schematic diagram to aid orientation of the sections by illustrating the location of various brain regions according to the Paxinos & Watson, 1986 rat brain atlas. Higher magnifications of Kv3.1b immunoreactivity in selected areas are illustrated in *B*–*G*. *B*, numerous neurones were labelled in the cuneate nucleus. *C*, all neurones in the gracile nucleus contained Kv3.1b-IR. *D*, a large Kv3.1b-IR neurone in the dorsal medullary reticular nucleus. *E*, example of a rare labelled neurone within the nucleus ambiguus (filled arrow). Also shown is a vagal preganglionic neurone (open arrow) which was identified by retrograde tracing with fluorogold (not shown). Typically, the vagal preganglionic neurone is apposed by Kv3.1b-immunoreactive structures, but does not contain the channel itself. *F*, Kv3.1b-IR neurones from the spinal trigeminal nucleus. *G*, a large presumptive motorneurone in the hypoglossal nucleus (XII) that is apposed by Kv3.1b-IR structures, but does not appear to contain the subunit within its membrane. Punctate Kv3.1b immunoreactivity is also present throughout the neuropil. AP, area postrema; cu, cuneate fasiculus; Cu, cuneate nucleus; DVN, dorsal vagal motor nucleus; Gr gracile nucleus; Lrt, lateral reticular nucleus; MdD, dorsal medullary reticular nucleus; MdV, ventral medullary reticular nucleus; NA, nucleus ambiguus; NTS, nucleus tractus solitarii; py, pyramidal tract; PMn, paramedian reticular nucleus; sp5, spinal trigeminal tract; Sp5, spinal trigeminal nucleus.

the commissural and medial subdivisions of the nucleus and within the TS (Fig. 2*A*). More rostrally, a greater number of Kv3.1b-IR cells were present in the medial, dorsolateral, interstitial and ventrolateral subdivisions and within the TS (Fig. 2*B* and *C*). Kv3.1b-IR neurones were approximately 36% of NeuN-IR cells in these areas (111/309 NeuN cells, 36%). However, since it was sometimes difficult to differentiate whether NTS neurones themselves contained Kv3.1b-IR or were closely apposed by Kv3.1b-IR structures, this analysis of colocalization is likely to be an underestimate.

At the light microscope level, Kv3.1b-IR NTS cells contained reaction product which was predominantly located close to the cell membrane of the soma and proximal dendrites, similar to that observed in the other areas of the medulla. Ultrastructural examination of such Kv3.1b-IR neurones revealed that Kv3.1b reaction product was indeed located close to the somatic and proximal dendritic membranes indicating that the channel is membrane bound (Fig. 2*D*). Kv3.1b reaction product observed in the cytoplasm of labelled NTS neurones may represent channels being transported to or from the plasma membranes, as it was often detected near to cellular structures such as the Golgi apparatus (Fig. 2*D*).

Both GABA-IR and Glut-IR cells in the proximity of the tractus contained Kv3.1b-IR (Fig. 3*A*–*D*). In addition, VGLUT2 or GAD_{65} mRNA was detected in Kv3.1b-IR cells (Fig. 3*E*–*H*). Since immunohistochemistry for GABA and glutamate in the NTS may provide either false-negative or false-positive results (Fremeau *et al.* 2002; Kaneko & Fujiyama, 2002), and *in situ* markedly reduced the number of visible Kv3.1b-IR neurones, we did not quantify the degree of colocalization in either case.

Electrophysiology indicates that Kv3.1-containing channels contribute to action potential repolarization and firing frequency of some NTS neurones

Whole-cell patch-clamp recordings were obtained from 102 neurones in the ventral aspect of the TS at the level of the area postrema. This area was targetted due to the relatively high density of Kv3.1b-IR neurones in the NTS. In addition, large neurones with proximal dendrites running in the mediolateral plane were preferentially selected (Fig. 2*E*) as this corresponds to the morphology of Kv3.1b-IR neurones. A total of 81/102 neurones displayed electrophysiological characteristics which may be supported by the presence of the Kv3.1b subunit (Table 1): rapid action potentials, high firing frequencies

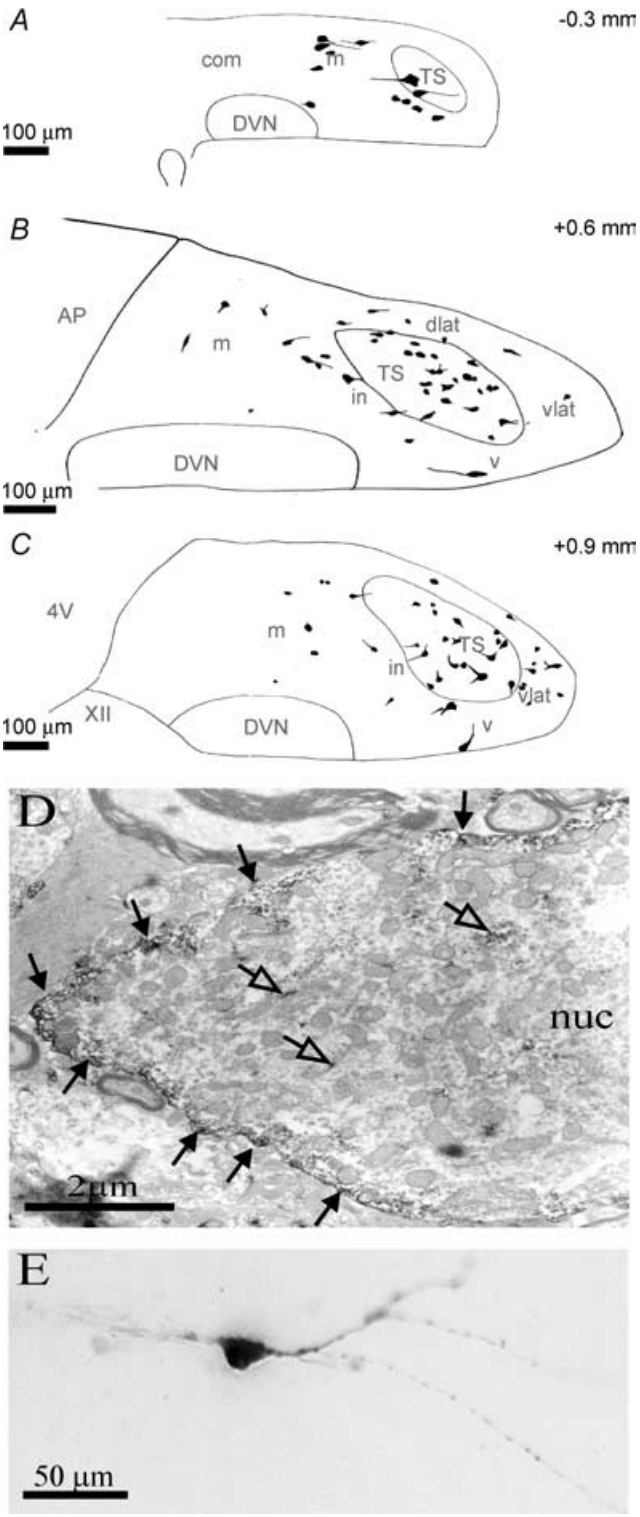

Figure 2. Kv3.1b-immunoreactive neurones in the NTS are located predominantly in the vicinity of the solitary tract
A–C, camera lucida drawings of Kv3.1b-immunoreactive neurones superimposed on sketches of NTS sections from three different rostrocaudal levels with respect to the obex (levels in top right hand corner). *A*, at caudal levels (at the level of the central canal) a few Kv3.1b-IR neurones were observed in the medial (m) subdivision of the NTS and within the tractus solitarius (TS). *B*, at the level of the area postrema (AP), a greater number of Kv3.1b-IR cells were present. A few Kv3.1b-IR neurones were located in the medial subnucleus, but a greater proportion were located in the dorsolateral (dLat), interstitial (in), ventral (v) and ventrolateral (vlat) subdivisions and within the TS. *C*, at the level of the fourth ventricle (4V), a similar distribution of Kv3.1b-IR neurones was observed to that at the level of the area postrema. Again, a few Kv3.1b-IR neurones were located in the medial subnucleus, but a greater proportion were located in the dLat, in, v and vlat subdivisions and within the TS. *D*, electron micrograph of a Kv3.1b-IR neurone in the NTS visualized with diaminobenzidine. The Kv3.1b reaction product is apposed to the membrane (filled arrows), suggesting that the channel is inserted into the membrane. Immunoreactivity is also sparsely distributed throughout the cytoplasm (open arrows); nuc, nucleus. *E*, NTS neurone filled with Lucifer yellow which was sensitive to TEA and 4-AP. The neurone was located in the ventral region of the tractus and the projections run in the mediolateral axis.

and sensitivity to TEA and 4-AP represented by increases in action potential duration (TEA, 4.6 ± 0.5 to 10.4 ± 1.5 ms; 4-AP, 4.2 ± 0.8 to 10.9 ± 1.2 ms; $P < 0.05$, $n = 81$; Fig. 4*A*, *B* and *F*). This effect was due to the repolarization phase being prolonged, and these pharmacological agents also reduced the AHP amplitude (TEA, 16.4 ± 1.3 to 11.9 ± 3 mV; 4-AP, 15.6 ± 1.1 to 10.9 ± 0.8 mV; $P < 0.05$; Fig. 4*A*, *B* and *F*). As a negative control, 14 neurones located in the DVN, which do not contain Kv3.1b immunoreactivity (Figs 1 and 6*C*), did not respond to the same concentrations of TEA (action potential duration: pre-TEA, 5.4 ± 0.9 ms; post-TEA, 5.4 ± 1.2 ms; AHP amplitude: pre-TEA, 17.9 ± 6.7 mV; post-TEA 17.7 ± 5.6 mV; $n = 14$, $P =$ n.s.; Fig. 4*C*) or 4-AP (action potential duration: pre-4-AP, 5.3 ± 1.3 ms; post-4-AP 5.3 ± 1.1 ms; AHP amplitude: pre-4-AP, 18.6 ± 7.5 mV; post-4-AP 18.5 ± 5.3 mV; $P =$ n.s.; Fig. 4*D*).

Whilst the blockade of many K^+ channels increases the firing rate of fast-spiking neurones, blockade of Kv3 channels decreases the firing frequency (Erisir *et al.* 1999). We therefore examined the effects of 4-AP and TEA on neuronal firing frequency. As well as the effects on individual action potentials, 4-AP and TEA reduced the firing frequencies of sensitive NTS neurones (Fig. 4*E*). In response to a current pulse of +150 pA, 4-AP reduced the instantaneous firing frequency from 66.1 ± 4.5 to 59.4 ± 3.3 Hz ($P < 0.05$), while the steady state decreased from 65.1 ± 2.1 to 57.4 ± 1.9 Hz ($P < 0.05$, $n = 12$). TEA also led to a decrease in both the instantaneous (66.8 ± 1.8 to 60.8 ± 2.3 Hz; $P < 0.05$) and steady-state (63.4 ± 1.7 to 58.3 ± 2.3 Hz, $P < 0.05$; $n = 19$) firing frequencies. Consistent with the absence of Kv3.1b-IR from DVN neurones, there was no effect of 4-AP or TEA on the firing frequency of DVN neurones ($n = 14$, data not shown).

Whilst the majority of 4-AP- and TEA-responsive neurones were located close to the solitary tract in ventral and ventrolateral regions, those that were unresponsive were predominantly localized more medially

towards the commissural NTS (Table 1). The 4-AP- and TEA-sensitive neurones displayed shorter action potential half-widths, larger AHP amplitude, higher instantaneous firing frequency and less late accommodation than those insensitive to 4-AP and TEA (Table 1).

The Kv3.1b subunit contributes to action potential repolarization and firing frequency of NTS neurones

Our electrophysiological studies with 4-AP and TEA are consistent with a Kv3.1-subunit-containing channel contributing to action potential repolarization in NTS neurones, supporting our immunohistochemical data that the Kv3.1b subunit was present in somata in the NTS. Previous studies have used Kv-subunit-specific antibodies to identify the subunit composition of ion channels, and there is growing evidence that these can have functional effects (Trimmer & Rhodes, 2004), which in expression systems commence within 8–10 min, and display time-dependent blockade (Murakoshi & Trimmer, 1999; Conforti *et al.* 2000), whilst first effects are observed with a longer time course in native cells (Archer *et al.* 1998; Lu *et al.* 2002; Sanchez *et al.* 2002). Since there is a lack of pharmacological tools that are selective for Kv3.1 isoforms, we sought to confirm the involvement of the Kv3.1b subunit in these cells by introducing the antibody to the inside of the cell via the patch pipette. Since the antibody is directed specifically against the intracellular C-terminus of the Kv3.1b subunit, our reasoning was that it would disrupt only channels containing the Kv3.1b subunit.

In NTS neurones, intracellular application of anti-Kv3.1b antibody resulted in progressive prolongation of the action potential duration (from 4.6 ± 0.7 to 7.7 ± 0.8 ms at 30 min; $P < 0.05$, $n = 7$; Fig. 5*A*). After 30 min, 4-AP could still produce a further significant increase in the action potential duration (7.7 ± 0.8 to 10.1 ± 1.1 ms; $P < 0.05$, $n = 7$), which was reversed upon washout of the 4-AP (Fig. 5*Ba*). However, repeated applications of 4-AP revealed a progressive blockade of 4-AP-sensitive channels due to the antibody, since at 65 min, 4-AP had no further effect on the action potential duration (11.2 ± 0.8 to 11.4 ± 0.7 ms; $P =$ n.s., $n = 7$; Fig. 5*Bb*). In addition, decreases were observed in instantaneous ($t = 0$ min, 61.5 ± 2.8 Hz; $t = 30$ min, 57 ± 2.5 Hz; $t = 60$ min, 54.8 ± 3 Hz; $P < 0.05$, $n = 7$) and steady-state ($t = 0$ min, 50.2 ± 3.2 Hz; $t = 30$ min, 45.5 ± 2.3 Hz; $t = 60$ min, 41.4 ± 2 Hz; $P < 0.05$, $n = 7$) firing frequencies as well as an increase in late accommodation ($t = 0$ min, $1.7 \pm 0.3\%$; $t = 30$ min, $5 \pm 0.6\%$; $t = 60$ min, $7.8 \pm 0.7\%$; $P < 0.05$, $n = 5$). There was no significant change in the input resistance ($t = 0$ min, 796 ± 41 MΩ; $t = 30$ min, 801 ± 39 MΩ; $n = 7$) or resting membrane potential ($t = 0$ min, 65.8 ± 5.1 mV; $t = 30$ min, 67.4 ± 6.3 mV; $n = 7$) during the time taken for the antibody to have an effect. There was no significant change in the duration of the action potential over the 60 min recording period when the antibody was not present ($t = 0$ min, 4.1 ± 0.2 ms; $t = 30$ min, 4.2 ± 0.4 ms; $t = 60$ min, 4.1 ± 0.4 ms;

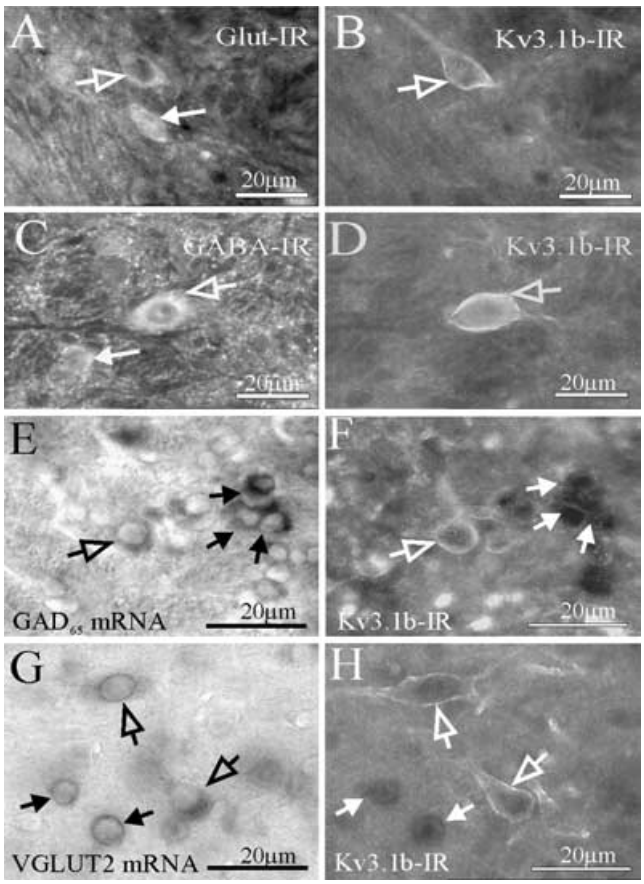

Figure 3. Kv3.1b immunoreactivity is present in both GABA- and glutamate-containing neurones in the NTS
A, two glutamate-immunoreactive neurones in the vicinity of the TS (arrows, visualized by Alexa^{488}). The open arrow points to one of the cells that is also Kv3.1b immunoreactive, as shown in *B*. *B*, same area as *A*, but viewed through a Cy3 filter set and showing a Kv3.1b-IR neurone (open arrow) that is also glutamate-IR as depicted in panel *A*. *C*, two GABA-IR neurones in the vicinity of the TS (arrows, visualized by Alexa^{488}). The open arrow highlights one of the cells that is also Kv3.1b-IR, as indicated in *D*. *D*, same area as *C*, but viewed through a Cy3 filter set, and showing a Kv3.1b-IR neurone (arrow) that is also GABA-IR, as depicted in *C*. *E*, neurones in the NTS expressing mRNA encoding the GAD_{65} isoform of the GABA-synthesizing enzyme glutamic acid decarboxylase (arrows). The open arrow highlights a labelled neurone that is also Kv3.1b-IR, as shown in *F*. *F*, visualization of the same region as in *E* with a Cy3 filter set to reveal Kv3.1b-IR indicates that one of the GAD_{65}-expressing neurones is also Kv3.1b-IR (open arrow). The other GAD_{65}-expressing neurones do not contain Kv3.1b-IR (filled arrows). *G*, neurones in the NTS expressing the mRNA for the vesicular glutamate transporter VGLUT2 (arrows). Two of these labelled neurones (open arrows) are also Kv3.1b-IR, as shown in *H*. Neurones indicated with filled arrows are not Kv3.1b-IR. *H*, visualizing Kv3.1b immunoreactivity in the same region as *G* reveals that two of the VGLUT2 expressing neurones are also Kv3.1b-IR (open arrows). Other VGLUT2-expressing neurones are not Kv3.1b-IR (filled arrows).

Table 1. Comparison of the intrinsic electrophysiological properties and location of 4-AP-/TEA-sensitive and insensitive neurones within the NTS

Parameter	4-AP-/TEA-responsive ($n = 81$)	Unresponsive ($n = 16$)	Level of significance
Location	Ventral/ventrolateral NTS	Commissural NTS	NA
RMP (mV)	69.5 ± 3.8	66.3 ± 5.7	n.s.
Input resistance (MΩ)	789 ± 96	954 ± 104	n.s.
Action potential duration (ms)	4.4 ± 1.2	7.2 ± 1.7	$P < 0.05$
AHP amplitude (mV)	16.1 ± 2.2	11.3 ± 2.7	$P < 0.05$
FF_{INST} (Hz)	66.9 ± 5.3	38.4 ± 4.3	$P < 0.05$
Early accommodation (%)	32.4 ± 3.3	39 ± 5.3	n.s.
Late accommodation (%)	$1.9 \pm 0.2\%$	$12.7 \pm 2.3\%$	$P < 0.05$

NA, not applicable; NTS, nucleus tractus solitarii; RMP, resting membrane potential; AHP, afterhyperpolarization; FF_{INST}.

$n = 10$, $P =$ n.s.; Fig. 4*A* and *B*). Action potentials, input resistance and resting membrane potentials of DVN neurones ($n = 7$), which do not contain Kv3.1b-IR (Figs 1*A* and 6*C*) yet contain Kv3.4-IR (Brooke *et al.* 2004*b*) were not affected by the presence of the Kv3.1b antibody (Fig. 6*A*).

Additionally, to test whether the effects of intracellular application of the Kv3.1b antibody to NTS neurones were not merely due to intracellular application of an antibody, we conducted the same experiments using an antibody raised against HCN1 which is rarely present in the NTS (Brooke *et al.* 2004*a*). Intracellular application of the HCN1 antibody at the same concentration as the Kv3.1b antibody, which is also the effective concentration for immunohistochemistry (Brooke *et al.* 2004*a*), did not significantly alter the action potential characteristics in NTS neurones (action potential duration: control, 4.0 ± 0.2 ms; HCN1 Ab, 4.2 ± 0.1 ms; AHP amplitude: control, 24.2 ± 1.3 mV; HCN1 Ab, 24.9 ± 1.3 mV; $P =$ n.s., $n = 6$; Fig. 5*C*) or DVN neurones (data not shown). The neurones located within the NTS were, however, still responsive to TEA following intracellular dialysis of the HCN1 antibody. As before, TEA led to a significant increase in the action potential duration and a decrease in the AHP, and was fully reversible on wash out (action potential duration: HCN1 Ab, 4.1 ± 0.1 ms; HCN1 Ab + TEA, 7.6 ± 0.2; $P < 0.05$; AHP amplitude: HCN1 Ab, 24.9 ± 1.4 mV; HCN1 Ab + TEA, 19.9 ± 0.9 mV; $P < 0.05$, $n = 6$; Fig. 5*C*). This indicates that introduction of the antibody intracellularly does not interfere with nonspecific targets.

As further verification that the Kv3.1b antibody was acting on Kv3.1b-containing channels, we recorded from neurones in the dorsal column nuclei (DCN), which all contained Kv3.1b-IR (Fig. 1*B* and *C*). In control recordings without antibody in the pipette DCN, neurones responded to TEA (2/2) and/or 4-AP (4/4) with an increase in action potential duration (4-AP, 2.1 ± 0.3 to 3 ± 0.1 ms; $P < 0.05$). When recordings were made with the antibody present in the pipette during the experiments the action potential duration progressively increased (AP duration: $t = 0$ min, 2 ± 0.2 ms; $t = 50$ min, 2.9 ± 0.3 ms; $P < 0.05$, $n = 4$; Fig. 5*Da*). During initial stages of recordings, 4-AP prolonged action potential duration similar to control cells (AP duration: $t = 15$ min, 2.3 ± 0.2 to 2.8 ± 0.1 ms; $P < 0.05$, $n = 4$; Fig. 5*Da*). However, after 50 min, 4-AP had no further effect (AP duration: 2.91 ± 0.2 to 2.93 ± 0.1 ms; $P =$ n.s., $n = 4$, Fig. 5*Db*).

We further tested whether the Kv3.1b antibody could be acting on other Kv3 subunits by intracellular application to cerebellar Purkinje neurones which contain Kv3.2 (Fig. 6*E*), Kv3.3 and Kv3.4 subunits (Weiser *et al.* 1994; Goldman-Wohl *et al.* 1994; Martina *et al.* 2003) but not Kv3.1b subunits (Fig. 6*D*; Weiser *et al.* 1995; Sekirnjak *et al.* 1997). The presence of the Kv3.1b antibody had no effect on the duration of the action potential (Fig. 6*B*), measured from first action potential at $t = 0$ min, 1.2 ± 0.04 ms; $t = 30$ min, 1.2 ± 0.03 ms; t = 60 min, 1.2 ± 0.04 ms; $P =$ n.s., $n = 6$) or amplitude of the AHP ($t = 0$ min, 21.2 ± 3.6 mV; $t = 30$ min, 20.8 ± 2.2 mV, $t = 60$ min 19.8 ± 2.3 mV; $n = 6$). TEA (100 μM) applied to three of these six cells increased the action potential duration (applied at $t = 45$ min, the duration increased from 1.2 ± 0.1 to 1.8 ± 0.2 ms), and this effect was reversed upon removal and wash of TEA (recovery upon 15 min washout = 1.3 ± 0.1 ms; Fig. 6*B*). This TEA-induced increase in action potential duration observed in the Purkinje neurones was consistent with previous studies (Sacco & Tempia, 2002). These data indicate that the Kv3.1b antibody did not interfere with the Kv3 channel subunits present in cerebellar Purkinje cells.

Voltage-clamp studies reveals a TEA-sensitive K^+ current in NTS neurones

To investigate the basic properties of, and provide further evidence for, the Kv3 current within NTS neurones, we conducted voltage-clamp experiments using outside-out

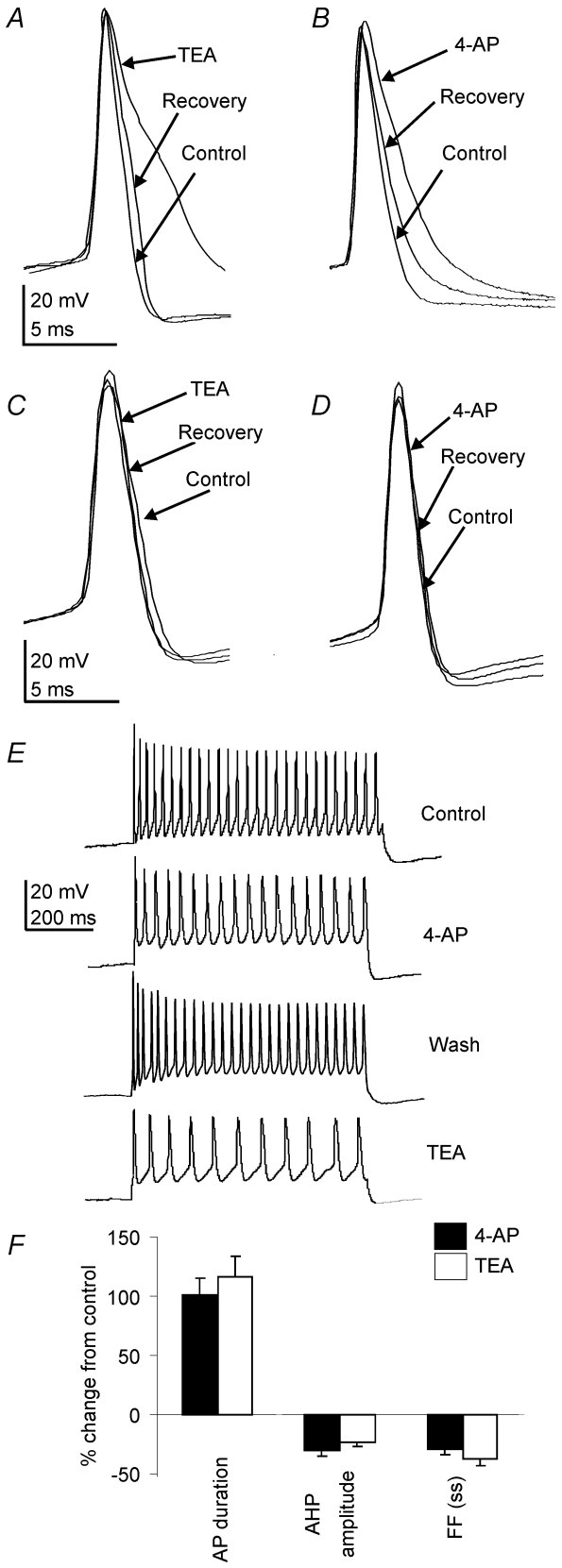

Figure 4. Low concentrations of TEA and 4-AP prolong repolarization of action potentials in NTS neurones
A, application of 0.5 mM TEA to an NTS neurone increased the action potential duration by prolonging the repolarization phase, an effect that was reversed on washout. *B*, application of 30 μM 4-AP to the same NTS neurone as in *A* similarly increased the action potential duration, and the effect was reversed on washout. These data were collected 1.5 h into the recording. Note the control action potential did not change from that in *A*, recorded at 25 min. *C* and *D*, examples of DVN neurones where 0.5 mM TEA (*C*) and 30 μM 4-AP (*D*) used at the same concentrations as on NTS neurones had no significant effect on the action potential duration. *E*, application of 4-AP to an NTS neurone reduced the number of action potentials fired in response to a +60 pA current pulse by 33%, an effect reversed on washout. Application of TEA to the same neurone also reduced the number of action potentials elicited (59% reduction). *F*, pooled data showing the effects of 4-AP and TEA on the action potential duration, afterhyperpolarization (AHP) amplitude and the steady-state firing frequency in NTS neurones as a percentage change from the control state.

patches in the presence of 100 nM α-DTX to block Kv1-subunit-containing channels (Coetzee *et al.* 1999). Somatic outside-out patches were excised within 30 s of establishing the whole-cell configuration, and were held at a holding potential of −110 mV. Depolarizing voltage steps to +30 mV (10 mV increments, 100 ms duration) revealed a voltage-dependent outward current (Fig. 7*A*, upper trace). All patches yielded a significant outward current of at least 200 pA when stepped to +30 mV. The steady-state outward current had a mean amplitude of 719 ± 114 pA ($n = 8$) for a voltage step to +30 mV. The mean maximum conductance was 8.1 ± 0.7 nS ($n = 8$). Initial trials indicated that we were unable to maintain high-resistance seals and satisfactory voltage control for sufficient durations when the antibody was present in the pipette and, therefore, we used pharmacological manipulations to isolate Kv3 currents, as previously reported (e.g. Coetzee *et al.* 1999; Southan & Robertson, 2000).

In the presence of α-DTX, TEA was applied to patches at a concentration of 100 μM, which is known to block Kv3-subunit-containing channels (Coetzee *et al.* 1999). All patches were sensitive to TEA at this concentration ($n = 8$), and a reduction in the total outward K^+ current was observed (48.4 ± 6.5%, $n = 6/6$ α-DTX-sensitive patches). Recovery (>60%) was observed following washout of TEA in all patches. Offline digital subtraction revealed the TEA-sensitive component (mean steady amplitude 414 ± 132 pA; $n = 6$), which activated in a voltage-dependent manner from a threshold of around −30 mV (Fig. 7*A*, lower trace). K^+ conductance–voltage curves of the TEA-sensitive current were fitted with a single, first-order Boltzmann function, yielding a mean $V_{½}$ of 0.1 ± 5.3 mV, and slope factor of 10.1 ± 2.2 mV ($n = 5$; Fig. 7*B*). The kinetics of this α-DTX-insensitive, TEA-sensitive current correlate with those previously published for Kv3-containing channels in both expression systems and native neurones (see Rudy *et al.* 1999; Lien & Jonas, 2003; Baranauskas *et al.* 2003; McCrossan *et al.* 2003).

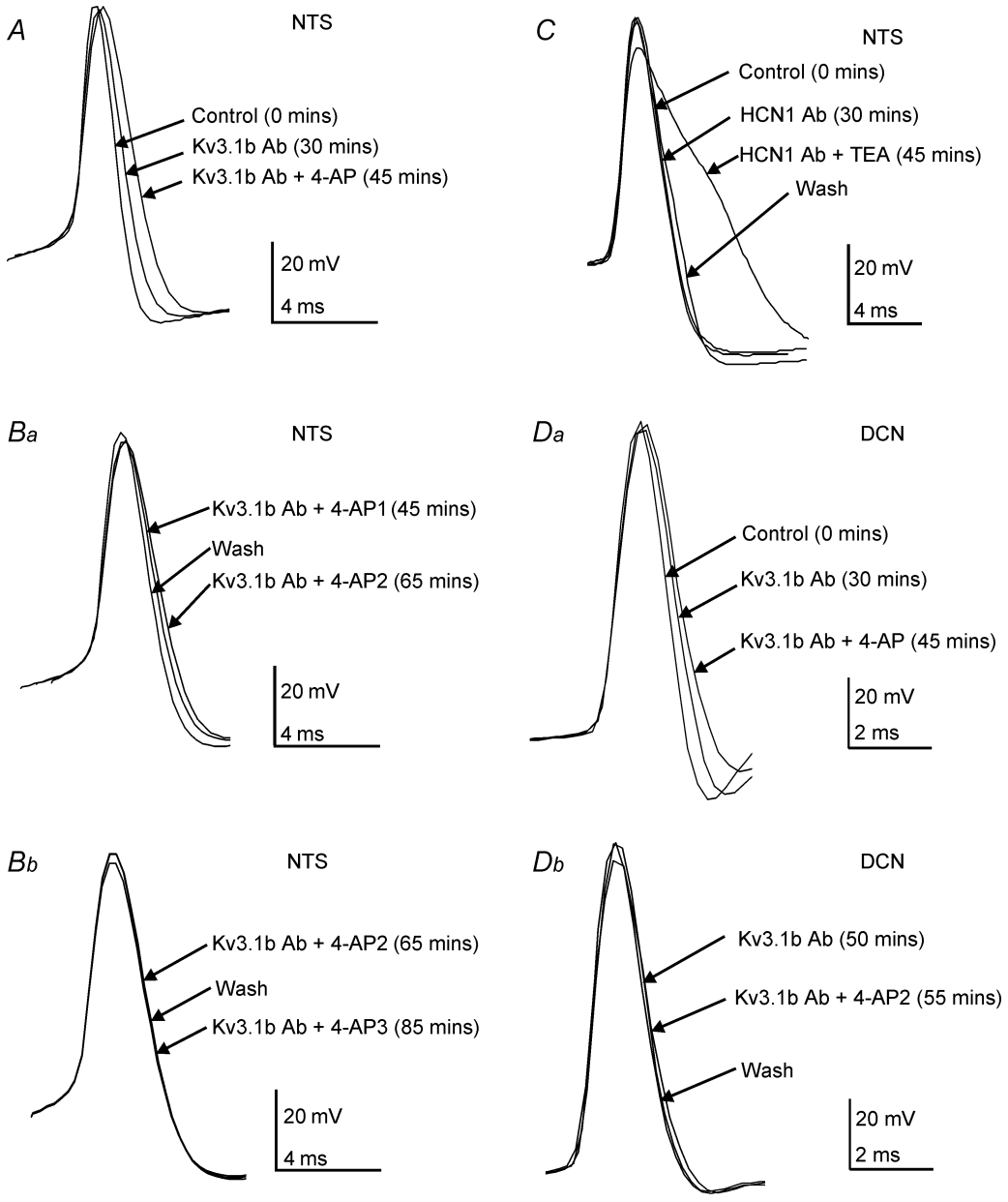

Figure 5. Intracellular application of an anti-Kv3.1b antibody, but not anti-HCN1, prolongs the action potential duration in neurones in the NTS
A, when an anti-Kv3.1b antibody (0.3 μg ml^{-1}) was present in the patch pipette, the action potential duration of the recorded NTS neurone increased gradually over time. This duration was further increased by subsequent application of 30 μM 4-AP. *Ba*, The same neurone as in *A* at a later time point. The effect of 4-AP (4-AP1) was partially reversed on washout and further application of 4-AP (4-AP2) prolonged the action potential duration as before. *Bb*, further application of 4-AP (4-AP3) at 85 min did not increase the action potential duration from that of the previous application (4-AP2), suggesting that the antibody had completely occluded the effects of 4-AP. *C*, example of an NTS neurone in which the hyperpolarization-activated cyclic nucleotide-gated channel 1 subunit (HCN1) antibody was added to the intracellular solution at the same concentration as the Kv3.1b antibody (0.3 μg ml^{-1}). The antibody alone had no effect on the action potential waveform, and did not alter the sensitivity to TEA (100 μM). *Da*, example of a DCN neurone in which intracellular application of the Kv3.1b antibody led to a progressive increase in the action potential duration, and this was further prolonged by bath application of 4-AP (30 μM). *Db*, the effect of 4-AP was occluded, since at $t = 50$ min, 4-AP (4-AP2) had no further effect on the action potential duration.

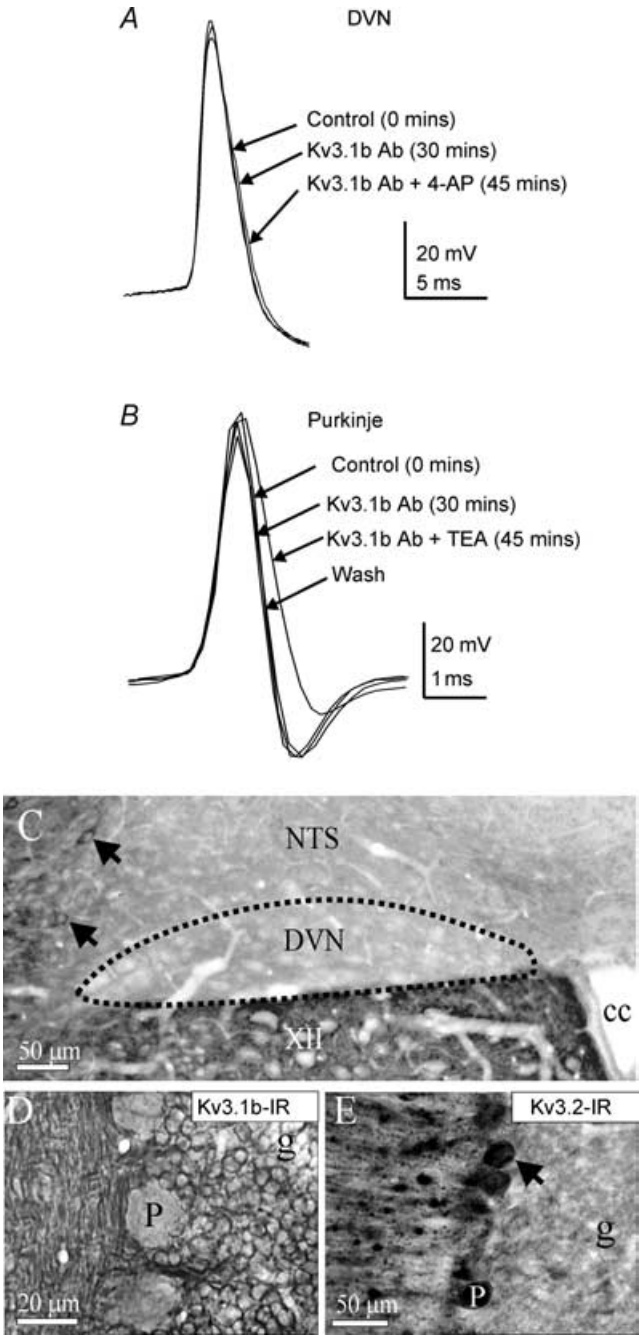

Figure 6. Intracellular application of the Kv3.1b antibody does not affect neurones which do not contain Kv3.1b, but which do contain other Kv3 subunits
A, in this DVN neurone, intracellular application of the Kv3.1b antibody and 30 μM 4-AP did not affect the action potential waveform. *B*, example of a cerebellar Purkinje neurone in which application of the Kv3.1b antibody did not affect the action potential shape, and did not interfere with sensitivity of the neurone to TEA (100 μM), presumably acting on the other Kv3 subunits in these cells. *C*, low-power image showing that Kv3.1b-IR (detected using DAB) is absent from the DVN. Labelled Kv3.1b-IR cells can clearly be seen in the interstitial region of the NTS (arrows), and punctate Kv3.1b-IR can also be observed in the hypoglossal nucleus (XII) in the same section; cc, central canal. *D*, high-power light microscope image showing Kv3.1b-IR is absent from cerebellar Purkinje cell somata. *E*, low-power light micrograph showing Kv3.2-IR is present in cerebellar Purkinje cell soma.

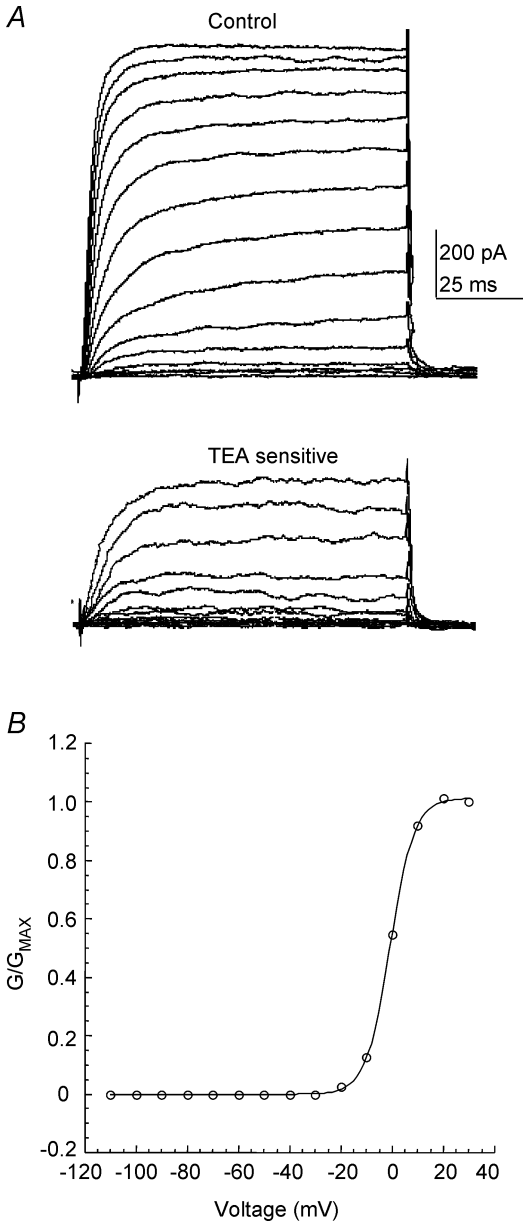

Figure 7. TEA-sensitive K^+ currents in α-DTX-sensitive outside-out patches from NTS neurones
A, upper panel, representative example of voltage-dependent K^+ currents recorded from an outside-out patch excised from an NTS neurone in response to 100 ms depolarizing voltage steps (in 10 mV increments) from a holding potential of −110 mV. Lower panel, offline digital subtraction of the current in the presence of TEA (100 μM; not shown) from the control current (*A*) reveals a TEA-sensitive component. *B*, representative example of the steady-state activation curve for the TEA-sensitive current. Data points were obtained by calculating the conductance of the TEA-sensitive component and plotting normalized values against the voltage step. A single, first-order Boltzmann function (see Methods for equation) is superimposed on the data points. Notice the threshold of around −20 mV, and the depolarized $V_{1/2}$ value.

Kv3.1b immunoreactivity is present in presynaptic terminals in the NTS, some of which are vagal afferent in origin

Ultrastructural examination revealed Kv3.1b-IR in numerous axons running in the TS (Fig. 8*B*) and presynaptic terminals ($n = 35$) in the NTS. These labelled terminals appeared to be restricted to the levels more rostral to the area postrema in the medial area of the NTS, and they formed synapses of both the symmetric and asymmetric type with Kv3.1b-labelled and unlabelled dendrites within this region (Fig. 8*A*, *C* and *D*). In the majority of Kv3.1b-IR terminals detected with DAB, the reaction product was often restricted to discrete zones within the terminals, predominantly observed close to the membrane, yet often distant to the active zone of the synapse (Fig. 8*A*). In addition, vagal afferent fibres detected by DAB formed synaptic contacts with Kv3.1b-gold-containing structures (Fig. 8*D*; $n = 9$).

At the ultrastructural level DAB labelled vagal afferent axons ($n = 25$; not shown) and vagal afferent terminals ($n = 15$; Fig. 8*C* and *D*) contained gold particles indicating they were Kv3.1b-IR. These double-labelled axons and terminals were principally present in the TS at the level of, and more rostral to, the area postrema, where they formed asymmetric-type synapses with Kv3.1b-containing dendritic structures as well as unlabelled dendrites. Kv3.1b-IR vagal afferent axons and terminals were observed in the same regions as vagal afferent structures which did not contain immunogold, indicating that the double labelling is not an artifact of the staining procedure.

Although the cell bodies giving rise to vagal afferent fibres in the NTS reside in the nodose ganglion, Kv3.1b-IR was present in the cytoplasm and not their somatic membrane (Fig. 8*E*; $n = 10$ nodose ganglia). Nevertheless, RT-PCR on nodose ganglion RNA revealed Kv3.1 transcripts (Fig. 8*F*). This represents an unusual organization of the Kv3.1b subunit since it appears to be targeted to the terminals of the afferent neurones, yet absent from their somata.

Pathway-specific enhancement of neurotransmitter release by 4-AP and TEA correlates with the presence of Kv3.1b.

Since we detected Kv3.1b in presynaptic terminals, we examined the effects of 4-AP and TEA on synaptic potentials evoked in NTS neurones. Electrical stimulation in the region of the TS, which contains vagal afferent axons and Kv3.1b-IR cells, elicited monosynaptic excitatory postsynaptic potentials (EPSPs) and inhibitory

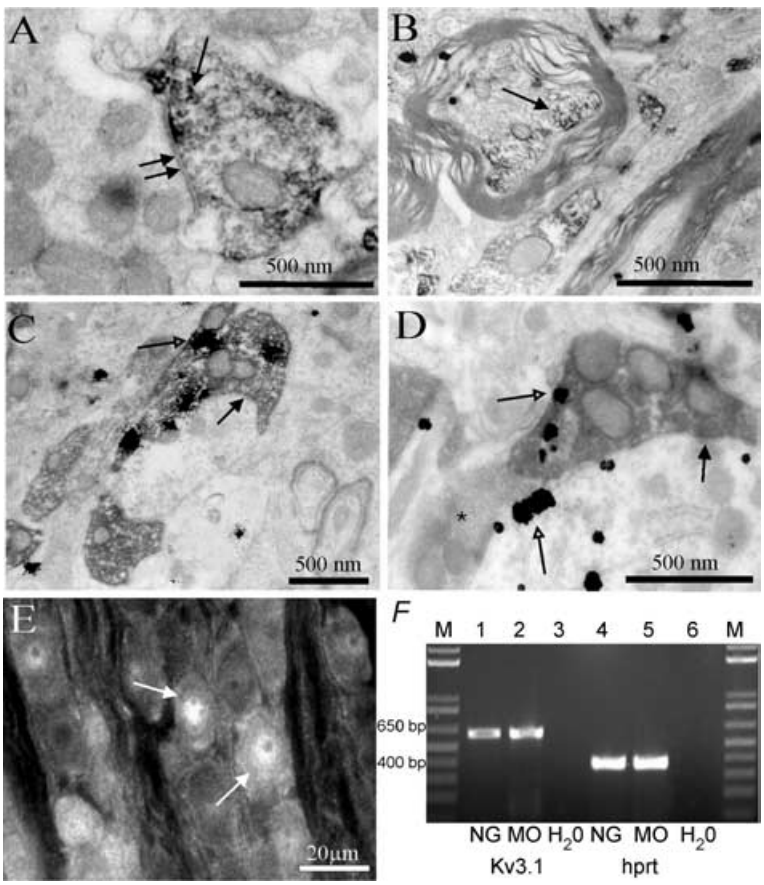

Figure 8. The Kv3.1b subunit is present in presynaptic terminals in the NTS, some of which are vagal afferent fibre terminals
A, electron micrograph of a Kv3.1b-immunoreactive terminal in the NTS identified by diaminobenzidine reaction product (arrow) that forms a synaptic contact (double arrows) with an unlabelled dendrite. *B*, a myelinated axon in the TS contains Kv3.1b immunoreactivity (arrow). *C*, a vagal afferent fibre terminal, identified by the presence of diaminobenzidine reaction product following detection of anterograde tracer injected into the nodose ganglion, makes synaptic contacts (double arrows) in the NTS. The terminal also contains silver-intensified gold (open arrow) indicating that it is Kv3.1b immunoreactive. *D*, an anterogradely labelled, Kv3.1b containing vagal afferent fibre terminal in the NTS forms a synaptic contact (filled arrow) with a Kv3.1b-immunoreactive neurone identified by silver-intensified gold particles (open arrows). An unlabelled terminal (asterisk) also innervates the same neurone. *E*, Kv3.1b immunoreactivity detected using a Cy3-conjugated secondary antibody in the nodose ganglion is present in the cytoplasm of some neurones, but absent from their membranes. The image has been transformed to greyscale and inverted. *F*, RT-PCR indicates that Kv3.1 is expressed in the nodose ganglion (NG; lane 1) and medulla oblongata (MO; lane 2). As a positive control for the PCR reaction, cDNA encoding the housekeeping gene *hprt* was amplified from RNA extracted from the NG (lane 4) and MO (lane 5). There were no amplified products detected when using water as a template (lanes 3 and 6). M, scale ladder.

postsynaptic potentials (IPSPs) in recorded NTS neurones (Fig. 9*A* and *B*). We considered these to be monosynaptic since they exhibited constant latency, all or nothing responses and a low failure rate in response to high-frequency stimulation (Neff *et al.* 1998; Doyle & Andresen, 2001). To determine if the effects of 4-AP and TEA were presynaptic, we examined the paired-pulse ratio (PPR), which is the ratio of the amplitude of the second EPSP compared to that of the first EPSP when two EPSPs are evoked in quick succession. If an effect is mediated postsynaptically, the ratio should remain unchanged, whereas a significant change in the PPR would be indicative of a presynaptic effect. Both 4-AP and TEA evoked increases in the amplitude of EPSPs elicited by both first (4-AP, $12.3 \pm 2.4\%$, $n = 28$; TEA, $28.3 \pm 3.1\%$, $n = 23$) and second (4-AP, $7.2 \pm 1.0\%$, $n = 28$; TEA, $10.8 \pm 1.8\%$, $n = 23$) stimuli (Fig. 9*A*). This was likely to be due to a presynaptic action since the PPR significantly decreased in the presence of 4-AP from 0.82 ± 0.01 to 0.73 ± 0.01, and with TEA from 0.78 ± 0.01 to 0.66 ± 0.01 (Fig. 9*A*; $P < 0.05$). IPSPs were also elicited by electrical stimulation of the TS and isolated by blockade of excitatory amino acid receptors using kynurenic acid (1 mM), as well as depolarizing the neurone to a holding potential of 0 mV. The amplitude of both IPSPs increased (Fig. 9*B*) with 4-AP (first, $23 \pm 2.8\%$; second, $11.3 \pm 1.4\%$; $n = 22$, $P < 0.05$) or TEA (first, $29.6 \pm 4.02\%$; second, $9.8 \pm 2.3\%$; $n = 20$, $P < 0.05$), and the PPR decreased with both compounds (4-AP, 0.7 ± 0.01 to 0.61 ± 0.02; TEA, 0.88 ± 0.02 to 0.65 ± 0.01). Postsynaptic membrane potential and input resistance did not change during these presynaptic experiments.

To determine if the effects of 4-AP and TEA correlated with the presence of Kv3.1b, we activated synaptic potentials in NTS neurones by stimulation of the reticular formation lateral to the hypoglossal nucleus, which does not contain Kv3.1b-IR. EPSPs and IPSPs elicited in NTS neurones by stimulation of this region were not affected (Fig. 9*C*) by 4-AP (EPSP, 6 ± 1.1 to 5.9 ± 0.5 mV, $n = 8$; IPSP, 5.2 ± 0.8 to 4.9 ± 0.7 mV, $n = 8$; $P =$ n.s.) or TEA (EPSP, 5.4 ± 0.8 to 5.0 ± 0.7 mV, $n = 8$; IPSP, 4.3 ± 0.7 to 4.5 ± 1.1 mV, $n = 6$; $P =$ n.s.). Therefore TEA and 4-AP enhanced release of neurotransmitter(s) only in the pathway where Kv3.1b-IR could be detected.

Discussion

In this study, neuroanatomical techniques revealed that Kv3.1b-IR is present in: (1) several neuronal populations in the medulla oblongata; (2) neuronal somata in the NTS which can be either GABA or glutamatergic in nature, and are predominantly restricted to the vicinity of the TS; (3) presynaptic terminals in the NTS, some of which are vagal afferent in origin, and also in NTS cells which receive vagal afferent input. Parallel *in vitro* electrophysiological experiments in the NTS revealed features consistent with the presence of Kv3.1 subunits in somata and terminals. NTS cells exhibited: (1) currents with characteristics of those mediated by Kv3.1 channels; (2) rapid action potentials and high firing frequencies sensitive to low concentrations of TEA and 4-AP; (3) evidence for specific involvement of Kv3.1b subunits since intracellular application of anti-Kv3.1b antibody mimicked and occluded the actions of low concentrations of TEA and

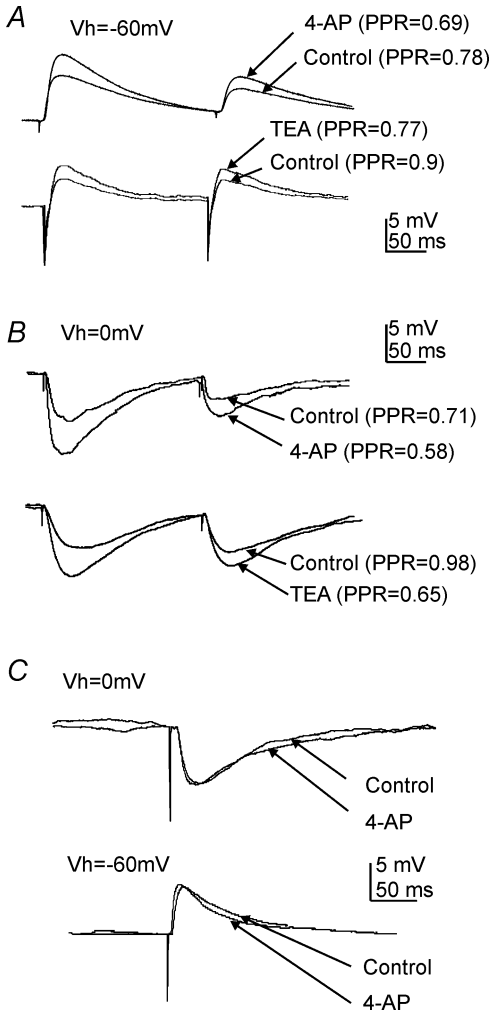

Figure 9. Pathway-specific modulation of neurotransmitter release by 4-AP and TEA in the NTS
A, paired stimulation of the solitary-tract-elicited EPSPs in an NTS neurone with a paired-pulse ratio (PPR) of 0.78. Application of 30 μM 4-AP (upper trace) increased the amplitude of both the first and second EPSPs, but significantly decreased the PPR to 0.69. Application of 0.5 mM TEA had a similar effect (lower trace). *B*, IPSPs in an NTS neurone evoked by paired-pulse stimulation of the solitary tract in the presence of kynurenic acid, and at a holding potential of 0 mV. Applications of both 4-AP (upper trace) and TEA (lower trace) increased IPSP amplitude and decreased the PPR. *C*, stimulation of the reticular formation in a region where Kv3.1b-immunoreactive neurones were not detected elicited EPSPs (upper trace) and IPSPs (lower trace) in NTS neurones on which 4-AP had no effect. All traces are averages of ten single sweeps.

4-AP; (4) modulation of their synaptic inputs by TEA and 4-AP in an input-specific manner that correlated with Kv3.1b-IR in the pathway.

Subunit selective disruption reveals that Kv3.1b subunits contribute to the shape of action potentials in NTS neurones

NTS cells that were sensitive to low concentrations of 4-AP and TEA had faster action potential kinetics and firing frequencies than insensitive neurones. Whilst overlapping sensitivity to both TEA and 4-AP is consistent with the presence of Kv3.1 subunits (Coetzee *et al.* 1999; Deuchars *et al.* 2001), the action potential duration and firing frequencies were lower than observed for other cells containing Kv3.1b subunits (e.g. Wang *et al.* 1998; Erisir *et al.* 1999). Nevertheless, our data provide direct evidence that Kv3.1b contributes to the action potential waveform, since intracellular application of anti-Kv3.1b antibody elicited effects likely to be specific to Kv3.1b subunits as: (1) the actions of the antibody mimicked and occluded the effects of TEA (100 μM) and 4-AP (30 μM), suggesting that they are acting on the same target; (2) action potentials of neurones in areas that do not contain Kv3.1b immunoreactivity (dorsal vagal nucleus and cerebellar Purkinje neurones) were unaffected, while it was effective in all cells in the dorsal column nuclei, which all contained Kv3.1b-IR – thus the presence of Kv3.1b correlates with the antibody action; (3) the antibody did not act on other Kv3 subunits since the action potential characteristics of cells containing Kv3.4 (dorsal vagal neurones, Brooke *et al.* 2003, 2004*b*) or Kv3.2, 3.3 and 3.4 subunits (cerebellar Purkinje cells, Martina *et al.* 2003) were not affected by the antibody – these experiments also show that the antibody does not affect the wide variety of channels (e.g. Na^+ and other K^+ channels) determining action potential waveform in cells that do not contain Kv3.1b; (4) the effects of anti-Kv3.1b antibody are not due to a non-specific interaction of the antibody with cellular machinery since inclusion of an antibody directed against HCN1, another ion channel absent from these cells, had no effect; (5) finally, the regions in the NTS where we performed our electrophysiological recordings correlate with those that contained Kv3.1b-immunoreactive somata. The mechanism of action of the antibody could not be determined from these experiments, but possibilities include disruption of trafficking, changes of conformation or physical blockade of the pore. Nevertheless, the evidence accumulated here indicates that Kv3.1b subunits are highly likely to contribute to the firing patterns of these NTS cells. Since they do not fire as fast as other Kv3.1b-containing neurones, these slower firing rates may be a consequence of phosphorylation (Macica *et al.* 2003) and/or association with accessory subunits such as MiRP1/2 or MinK, which can modulate the rate of channel activation and deactivation without affecting 4-AP sensitivity (Lewis *et al.* 2003; McCrossan *et al.* 2003).

NTS neurones display a Kv3-like current

The currents recorded in voltage clamp also display properties consistent with those carried by Kv3-containing channels. For instance, a large proportion of the current was sensitive to low concentrations of TEA (in the presence of α-DTX); the activation curve for the TEA-sensitive current had a threshold of around −30 mV, and a half-activation voltage of around 0 mV. These features have all been observed in mammalian cell lines expressing Kv3-subunit-containing channels (Rudy *et al.* 1999) as well as neurones containing Kv3 channels in the CNS (Wang *et al.* 1998; Erisir *et al.* 1999; Hernandez-Pineda *et al.* 1999; Baranauskas *et al.* 2003; Martina *et al.* 2003). At this stage we are unable to rule out the possibility that association with accessory subunits may alter the biophysical properties of the Kv3 channels expressed in NTS neurones (Lewis *et al.* 2003; McCrossan *et al.* 2003).

Potential role of presynaptic Kv3.1 subunits in neurotransmitter release in the NTS

While Kv3.1 subunits have previously been identified in presynaptic terminals (Sekirnjak *et al.* 1997; Wang *et al.* 1998; Parameshwaran *et al.* 2001; Ozaita *et al.* 2002; Ishikawa *et al.* 2003), their physiological role in this location has been rarely addressed. It is known that terminals can display currents typical of Kv3 channels since direct recordings from presynaptic 'pinceau' terminals in the cerebellum revealed a dendrotoxin-resistant, TEA-sensitive current (Southan & Robertson, 2000); however, these terminals contain only Kv3.4 (Laube *et al.* 1996) and possibly Kv3.3 (Taylor & Perney, 2001; McMahon *et al.* 2004) channel subunits. Kv3.1b subunits have been detected in terminals of the calyx of Held, where neurotransmitter release is regulated by a Kv3 channel (Ishikawa *et al.* 2003). The terminals in the NTS are too small for direct patch-clamp recordings, and we therefore used the paired-pulse protocol as an indirect measure of terminal function and neurotransmitter release (Clements, 1990). Consistent with blockade of a K^+ channel, we found that low concentrations of TEA and 4-AP (likely to act on Kv3.1 subunits, Coetzee *et al.* 1999; Deuchars *et al.* 2001) increased release of neurotransmitter, as reflected in a decrease in PPR. However, this effect was observed only in a pathway where Kv3.1b-IR was detected (TS), and not in a control pathway lacking Kv3.1b-IR (reticular formation). Although the electrophysiological data correlate well with immunohistochemistry, we were

limited to an indirect measurement, and there remains the possibility that even the low concentrations of TEA and 4-AP used may act on other channels that affect transmitter release. In particular, we cannot exclude a contribution from Kv3.1a subunits, since these appear to be trafficked preferentially to terminals of neurones in other CNS regions (Ozaita *et al.* 2002). The two splice variants exhibit similar currents and sensitivity to TEA and 4-AP (Coetzee *et al.* 1999), thus, the effects observed could be due to blockade of a heteromeric complex of these two isoforms. In addition, it is possible that in these terminals, Kv3.1 subunits participate in heteromeric complexes with other Kv3 subunits such as Kv3.2 (Hernandez-Pineda *et al.* 1999; Tansey *et al.* 2002), Kv3.3 (Rudy *et al.* 1999) and Kv3.4 (Baranauskas *et al.* 2003) in other CNS regions. Neither studies of expression (Weiser *et al.* 1994) nor protein (L. Atkinson, unpublished results) detect Kv3.2 in the medulla oblongata, but Kv3.3 (J. Deuchars, unpublished results) and Kv3.4 (Brooke *et al.* 2004*b*) are present. Therefore, we can conclude that our data are consistent with the proposed role of Kv3 in regulation of transmitter release from the calyx of Held (Ishikawa *et al.* 2003).

Functional role of Kv3.1b in the NTS

In vivo, few functionally identified cell types in the NTS exhibit the fast-firing phenotype typical of Kv3.1b-containing neurones. Possible candidates include 'pump' neurones, which are driven by afferents from the pulmonary slowly adapting receptors, and may be part of the Hering–Breuer reflex (Berger, 1977). During prolonged lung inflation, these cells maintain high-frequency discharge with little or no adaptation (Kalia & Richter, 1985; Miyazaki *et al.* 1998). Consistent with this, Kv3.1b-IR NTS cells correspond in location, size and approximate orientation to pump neurones in the rat (Ezure *et al.* 2002). In addition, Kv3.1b cells contain markers for GAD or VGLUT2, and some pump cells can synaptically inhibit cells (Ezure & Tanaka, 2000), while others have been proposed to be excitatory, since respiratory neurones are excited by lung inflations (Hayashi *et al.* 1996). The Kv3.1b-IR vagal afferent terminals may therefore represent slowly adapting receptors from the lung since these also fire at high frequencies with little or no adaptation (Miyazaki *et al.* 1998). In support of this possibility, we observed Kv3.1b-IR vagal afferent terminals in synaptic contact with Kv3.1b-IR NTS neurones. Electrophysiologically, we also observed 4-AP-sensitive vagal afferent inputs to neurones in which the repolarization of the action potential was mediated by Kv3.1. The role of the Kv3.1b subunit in the NTS, similar to that in the auditory brainstem (Brew & Forsythe, 1995; Wang *et al.* 1998), may therefore be to facilitate high-frequency discharge and phase-lock cell activity to enable faithful distribution of the lung inflation signal throughout the appropriate circuitry.

Functional role of Kv3.1b in other regions of the medulla oblongata

Throughout the CNS, the Kv3.1b subunit imparts fast firing properties to neurones which are critical for the pattern of activity in neuronal circuits (Rudy & McBain, 2001). Here we have shown that the Kv3.1b subunit is present in many neurones of the medulla oblongata that we speculate may be interneurones. For example, in the nucleus ambiguus, the origin of vagal and glossopharyngeal projections to supra-diaphragmatic structures (Bieger & Hopkins, 1987), Kv3.1b-IR was absent from the efferent neurones themselves, but present in neurones that surrounded this nucleus. Similarly, in the hypoglossal nucleus, the few Kv3.1b-IR neurones were not motoneurones. This is analogous to the situation in the spinal cord where sympathetic preganglionic neurones lack Kv3.1b-IR, yet presympathetic interneurones express the Kv3.1b subunit (Deuchars *et al.* 2001; Brooke *et al.* 2002). Since fast firing neurones, such as those containing Kv3.1b, may govern the activity of output neurones in other brain regions (Cobb *et al.* 1995), it will be of interest to determine the role of Kv3.1b neurones throughout the medulla in shaping the activity of neuronal circuits such as those regulating autonomic output.

References

Archer SL, Souil E, Dinh-Xuan AT, Schremmer B, Mercier JC, El Yaagoubi A, Nguyen-Huu L, Reeve HL & Hampl V (1998). Molecular identification of the role of voltage-gated K^+ channels Kv1.5 and Kv2.1 in hypoxic pulmonary vasoconstriction, and control of resting membrane potential in rat pulmonary artery myocytes. *J Clin Invest* **101**, 2319–2330.

Atkinson L & Deuchars J (2000). Distribution of Kv3.1b immunoreactivity in the dorsomedial medulla of the rat. *Proc Physiol Soc* **526.P**, 171*P*.

Baranauskas G, Tkatch T, Nagata K, Yeh JZ & Surmeier DJ (2003). Kv3.4 subunits enhance the repolarizing efficiency of Kv3.1 channels in fast-spiking neurons. *Nat Neurosci* **6**, 258–266.

Barraco R, El-Ridi M, Ergene E, Parizon M & Bradley D (1992). An atlas of the rat subpostremal nucleus tractus solitarius. *Brain Res Bull* **29**, 703.

Berger AJ (1977). Dorsal respiratory group neurons in the medulla of cat: spinal projections, responses to lung inflation and superior laryngeal nerve stimulation. *Brain Res* **135**, 231–254.

Bieger D & Hopkins DA (1987). Viscerotopic representation of the upper alimentary tract in the medulla oblongata in the rat: the nucleus ambiguus. *J Comp Neurol* **262**, 546–562.

Brew HM & Forsythe ID (1995). Two voltage-dependent K^+ conductances with complementary functions in postsynaptic integration at a central auditory synapse. *J Neurosci* **15**, 8011–8022.

Brooke RE, Atkinson L, Batten TFC, Deuchars SA & Deuchars J (2004*b*). Association of potassium channel Kv3.4 subunits with pre- and post-synaptic structures in brainstem and spinal cord. *Neuroscience* **126**, 1001–1010.

Brooke RE, Dallas ML, Deuchars SA & Deuchars J (2003). Kv3.4 potassium channel subunit immunoreactivity in presynaptic terminals in the brainstem and spinal cord and influence of BDS in neurotransmitter release. *Abstr Soc Neurosci 368.5*.

Brooke RE, Edwards IJ, Milligan CJ, Deuchars SA & Deuchars J (2004*a*). The HCN1 ion channel subunit is prominently expressed in somatodendritic domains of neurones in sensory and motor systems. *J Physiol* **555.P**, PC13.

Brooke RE, Pyner S, McLeish P, Buchan S, Deuchars J & Deuchars SA (2002). Spinal cord interneurones labelled transneuronally from the adrenal gland by a GFP-herpes virus construct contain the potassium channel subunit Kv3.1b. *Auton Neurosci* **98**, 45–50.

Chow A, Erisir A, Farb C, Nadal MS, Ozaita A, Lau D, Welker E & Rudy B (1999). K^+ channel expression distinguishes subpopulations of parvalbumin- and somatostatin-containing neocortical interneurons. *J Neurosci* **19**, 9332–9345.

Clements JD (1990). A statistical test for demonstrating a presynaptic site of action for a modulator of synaptic amplitude. *J Neurosci Methods* **31**, 75–88.

Cobb SR, Buhl EH, Halasy K, Paulsen O & Somogyi P (1995). Synchronization of neuronal activity in hippocampus by individual GABAergic interneurons. *Nature* **378**, 75–78.

Coetzee WA, Amarillo Y, Chiu J, Chow A, Lau D, McCormack T, Moreno H, Nadal MS, Ozaita A, Pountney D, Saganich M, Vega-Saenz de Miera E & Rudy B (1999). Molecular diversity of K^+ channels. *Ann N Y Acad Sci* **868**, 233–285.

Conforti L, Bodi I, Nisbet JW & Millhorn DE (2000). O_2-sensitive K^+ channels: role of the Kv1.2 subunit in mediating the hypoxic response. *J Physiol* **524**, 783–793.

Dallas ML, Deuchars SA, Lewis DI & Deuchars J (2002). Population of neurones within dorsal and dorsomedial regions of the nucleus of the solitary tract that are sensitive to 4-AP and TEA. *J Physiol* **544.P**, 33*P*.

Dallas ML, Deuchars SA, Lewis DI & Deuchars J (2004). Evidence that the Kv3.1b subunit isoform contributes to the action potential repolarisation in neurones within the nucleus of the solitary tract in rat. *J Physiol* **555.P**, C32.

Deuchars SA, Brooke RE, Frater B & Deuchars J (2001). Properties of interneurones in the intermediolateral cell column of the rat spinal cord: role of the potassium channel subunit Kv3.1. *Neuroscience* **106**, 433–446.

Deuchars J, Li YW, Kasparov S & Paton JF (2000). Morphological and electrophysiological properties of neurones in the dorsal vagal complex of the rat activated by arterial baroreceptors. *J Comp Neurol* **417**, 233–249.

Doyle MW & Andresen MC (2001). Reliability of monosynaptic sensory transmission in brain stem neurons *in vitro*. *J Neurophysiol* **85**, 2213–2223.

Du J, Zhang L, Weiser M, Rudy B & McBain CJ (1996). Developmental expression and functional characterization of the potassium-channel subunit Kv3.1b in parvalbumin-containing interneurons of the rat hippocampus. *J Neurosci* **17**, 3136–3147.

Erisir A, Lau D, Rudy B & Leonard CS (1999). Function of specific K^+ channels in sustained high-frequency firing of fast-spiking neocortical interneurones. *J Neurophysiol* **82**, 2476–2489.

Esclapez M, Tillakaratne NJ, Tobin AJ & Houser CR (1993). Comparative localization of mRNAs encoding two forms of glutamic acid decarboxylase with nonradioactive *in situ* hybridization methods. *J Comp Neurol* **331**, 339–362.

Ezure K & Tanaka I (2000). Identification of deflation-sensitive inspiratory neurons in the dorsal respiratory group of the rat. *Brain Res* **883**, 22–30.

Ezure K, Tanaka I, Saito Y & Otake K (2002). Axonal projections of pulmonary slowly adapting receptor relay neurons in the rat. *J Comp Neurol* **446**, 81–94.

Fortin G & Champagnat J (1993). Spontaneous synaptic activities in rat nucleus tractus solitarius neurones in vitro: evidence for re-excitatory processing. *Brain Res* **630**, 125–135.

Goldman-Wohl DS, Chan E, Baird D & Heintz N (1994). Kv3.3b: a novel Shaw-type potassium channel expressed in terminally differentiated cerebellar Purkinje cells and deep cerebellar nuclei. *J Neurosci* **14**, 511–522.

Grissmer S, Nguyen AN, Aiyar J, Hanson DC, Mather RJ, Gutman GA, Karmilowicz MJ, Auperin DD & Chandy KG (1994). Pharmacological characterization of five cloned voltage-gated K^+ channels, types Kv1.1, 1.2, 1.3, 1.5, and 3.1, stably expressed in mammalian cell lines. *Mol Pharmacol* **45**, 1227–1234.

Haddad GG & Getting PA (1989). Repetitive firing properties of neurons in the ventral region of nucleus tractus solitarius. *In vitro* studies in adult and neonatal rat. *J Neurophysiol* **62**, 1213–1224.

Hayashi F, Coles SK & McCrimmon DR (1996). Respiratory neurons mediating the Breuer–Hering reflex prolongation of expiration in rat. *J Neurosci* **16**, 6526–6536.

Hernandez-Pineda R, Chow A, Amarillo Y, Moreno H, Saganich M, Vega-Saenz de Miera EC, Hernandez-Cruz A & Rudy B (1999). Kv3.1–Kv3.2 channels underlie a high-voltage-activating component of the delayed rectifier K^+ current in projecting neurons from the globus pallidus. *J Neurophysiol* **82**, 1512–1528.

Ishikawa T, Nakamura Y, Saitoh N, Li WB, Iwasaki S & Takahashi T (2003). Distinct roles of Kv1 and Kv3 potassium channels at the calyx of Held presynaptic terminal. *J Neurosci* **23**, 10445–10453.

Kalia M & Richter D (1985). Morphology of physiologically identified slowly adapting lung stretch receptor afferents stained with intra-axonal horseradish peroxidase in the nucleus of the tractus solitarius of the cat. I. A light microscopic analysis. *J Comp Neurol* **241**, 503–520.

Kaneko T & Fujiyama F (2002). Complementary distribution of vesicular glutamate transporters in the central nervous system. *Neurosci Res* **42**, 243–250.

Kanemasa T, Gan L, Perney TM, Wang LY & Kaczmarek LK (1995). Electrophysiological and pharmacological characterization of a mammalian Shaw channel expressed in NIH 3T3 fibroblasts. *J Neurophysiol* **74**, 207–217.

Kawai Y & Senba E (1996). Organization of excitatory and inhibitory local networks in the caudal nucleus of tractus solitarius of rats revealed in *in vitro* slice preparation. *J Comp Neurol* **373**, 309–321.

Kawai Y & Senba E (1999). Electrophysiological and morphological characterization of cytochemically defined neurones in the caudal nucleus of tractus solitarius of the rat. *Neuroscience* **89**, 1347–1355.

Laube G, Roper J, Pitt JC, Sewing S, Kistner U, Garner CC, Pongs O & Veh RW (1996). Ultrastructural localization of Shaker-related potassium channel subunits and synapse-associated protein 90 to septate-like junctions in rat cerebellar Pinceaux. *Brain Res Mol Brain Res* **42**, 51–61.

Lawrence AJ & Jarrott B (1996). Neurochemical modulation of cardiovascular control in the nucleus tractus solitarius. *Prog Neurobiol* **48**, 21–53.

Lewis A, McCrossan ZA & Abbott GW (2003). MinK, MiRP1 and MiRP2 diversify Kv3.1 and Kv3.2 potassium channel gating. *J Biol Chem* **279**, 7884–7892.

Lien CC & Jonas P (2003). Kv3 potassium conductance is necessary and kinetically optimized for high-frequency action potential generation in hippocampal interneurons. *J Neurosci* **23**, 2058–2068.

Lorincz A, Notomi T, Tamas G, Shigemoto R & Nusser Z (2002). Polarized and compartment-dependent distribution of HCN1 in pyramidal cell dendrites. *Nat Neurosci* **5**, 1185–1193.

Lu Y, Hannaq ST, Tang G & Wang R (2002). Contributions of Kv1.2, Kv1.5 and Kv2.1 subunits to the native delayed rectifier K^+ current in rat mesenteric artery smooth muscle cells. *Life Sci* **71**, 1465–1473.

Luneau CJ, Williams JB, Marshall J, Levitan ES, Oliva C, Smith JS, Antanavage J, Folander K, Stein RB, Swanson R, Kaczmarek L & Buhrow SA (1991). Alternative splicing contributes to K^+ channel diversity in the mammalian central nervous system. *Proc Natl Acad Sci U S A* **88**, 3932–3936.

Macica CM, von Hehn CA, Wang LY, Ho CS, Yokoyama S, Joho RH & Kaczmarek LK (2003). Modulation of the kv3.1b potassium channel isoform adjusts the fidelity of the firing pattern of auditory neurons. *J Neurosci* **23**, 1133–1141.

Maley BE (1996). Immunohistochemical localization of neuropeptides and neurotransmitters in the nucleus tractus solitarius. *Chem Senses* **21**, 367–376.

Martina M, Yao GL & Bean BP (2003). Properties and functional role of voltage-dependent potassium channels in dendrites of rat cerebellar Purkinje neurons. *J Neurosci* **23**, 5698–5707.

McCrossan ZA, Lewis A, Panaghie G, Jordan PN, Christini DJ, Lemer DJ & Abbott GW (2003). MinK-related peptide 2 modulates Kv2.1 and Kv3.1 potassium channels in mammalian brain. *J Neurosci* **23**, 8077–8091.

McMahon A, Fowler SC, Perney TM, Akemann W, Knopfel T & Joho RH (2004). Allele-dependent changes of olivocerebellar circuit properties in the absence of the voltage-gated potassium channels Kv3.1 and Kv3.3. *Eur J Neurosci* **19**, 3317–3327.

Miyazaki M, Arata A, Tanaka I & Ezure K (1998). Activity of rat pump neurons is modulated with central respiratory rhythm. *Neurosci Lett* **249**, 61–64.

Murakoshi H & Trimmer JS (1999). Identification of the Kv2.1 K^+ channel as a major component of the delayed rectifier K^+ current in rat hippocampal neurons. *J Neurosci* **19**, 1728–1735.

Neff RA, Mihalevich M & Mendelowitz D (1998). Stimulation of NTS activates NMDA and non-NMDA receptors in rat cardiac vagal neurons in the nucleus ambiguus. *Brain Res* **792**, 277–282.

Ozaita A, Martone ME, Ellisman MH & Rudy B (2002). Differential subcellular localization of the two alternatively spliced isoforms of the Kv3.1 potassium channel subunit in the brain. *J Neurophysiol* **88**, 394–408.

Parameshwaran S, Carr CE & Perney TM (2001). Expression of the Kv3.1 potassium channel in the avian auditory brainstem. *J Neurosci* **21**, 485–494.

Paxinos G & Watson C (1986). *The Rat Brain in Stereotaxic Co-ordinates*, 2nd edn. Academic Press, San Diego, USA.

Rudy B, Chow A, Lau D, Amarillo Y, Ozaita A, Saganich M, Moreno H, Nadal MS, Hernandez-Pineda R, Hernandez-Cruz A, Erisir A, Leonard C & Vega-Saenz de Miera E (1999). Contributions of Kv3 channels to neuronal excitability. *Ann N Y Acad Sci* **868**, 304–343.

Rudy B & McBain CJ (2001). Kv3 channels: voltage gated K^+ channels designed for high-frequency repetitive firing. *Trends Neurosci* **24**, 517–526.

Sacco T & Tempia F (2002). A-type potassium currents active at subthreshold potentials in mouse cerebellar Purkinje cells. *J Physiol* **543**, 505–520.

Sanchez D, Lopez-Lopez JR, Perez-Garcia MT, Sanz-Alfayate G, Obeso A, Ganfornina MD & Gonzalez C (2002). Molecular identification of Kvalpha subunits that contribute to the oxygen-sensitive K^+ current of chemoreceptor cells of the rabbit carotid body. *J Physiol* **542**, 369–382.

Sekirnjak C, Martone ME, Weiser M, Deerinck T, Bueno E, Rudy B & Ellisman M (1997). Subcellular localization of the K^+ channel subunit Kv3.1b in selected rat CNS neurons. *Brain Res* **766**, 173–187.

Southan AP & Robertson B (2000). Electrophysiological characterization of voltage-gated K^+ currents in cerebellar basket and Purkinje cells: Kv1 and Kv3 channel subfamilies are present in basket cell nerve terminals. *J Neurosci* **20**, 114–122.

Stornetta RL, Sevigny CP & Guyenet PG (2002). Vesicular glutamate transporter DNPI/VGLUT2 mRNA is present in C1 and several other groups of brainstem catecholaminergic neurons. *J Comp Neurol* **444**, 191–206.

Tansey EP, Chow A, Rudy B & McBain CJ (2002). Developmental expression of potassium-channel subunit Kv3.2 within subpopulations of mouse hippocampal inhibitory interneurons. *Hippocampus* **12**, 137–148.

Taylor LA & Perney TM (2001). Immunohistochemical characterization of Kv3.3 potassium channel subunit distribution in the brain. *Abstr Soc Neurosci* 708.16.

Traub RD, Jefferys JG & Whittington MA (1999). Functionally relevant and functionally disruptive (epileptic) synchronized oscillations in brain slices. *Adv Neurol* **79**, 709–724.

Trimmer JS & Rhodes KJ (2004). Localization of voltage-gated ion channels in mammalian brain. *Annu Rev Physiol* **66**, 477–519.

Wang LY, Gan L, Forsythe ID & Kaczmarek LK (1998). Contribution of the Kv3.1 potassium channel to high-frequency firing in mouse auditory neurones. *J Physiol* **509**, 183–194.

Weiser M, Bueno E, Sekirnjak C, Martone ME, Baker H, Hillman D, Chen S, Thornhill W, Ellisman M & Rudy B (1995). The potassium channel subunit Kv3.1b is localized to somatic and axonal membranes of specific populations of CNS neurons. *J Neurosci* **15**, 4298–4314.

Weiser M, Vega-Saenz dM, Kentros C, Moreno H, Franzen L, Hillman D, Baker H & Rudy B (1994). Differential expression of Shaw-related K^+ channels in the rat central nervous system. *J Neurosci* **14**, 949–972.

Wuenschell CW, Fisher RS, Kaufman DL & Tobin AJ (1986). *In situ* hybridization to localize mRNA encoding the neurotransmitter synthetic enzyme glutamate decarboxylase in mouse cerebellum. *Proc Natl Acad Sci U S A* **83**, 6193–6197.

Acknowledgements

We thank the Wellcome Trust (L.A., C.J.M., J.D.) and British Heart Foundation (S.A.D, J.D.) for funding. We are grateful to Ruth L. Stornetta (University of Virginia) for the VGLUT2 *in situ* hybridization probes and discussion on protocols, Drs Niranjala Tillakaratne and A. J. Tobin (University of California) for the GAD cDNA probes.